Signal Transduction by Different Forms of the γδ T Cell–Specific Pattern Recognition Receptor WC1

Chuang Chen,*,[1] Haoting Hsu,*,† Edward Hudgens,* Janice C. Telfer,*,† and Cynthia L. Baldwin*,†

WC1 coreceptors are scavenger receptor cysteine-rich (SRCR) family members, related to T19 in sheep, SCART in mice, and CD163c-α in humans, and form a 13-member subfamily in cattle exclusively expressed on γδ T cells. Subpopulations of γδ T cells are defined by anti-WC1 mAbs and respond to different pathogen species accordingly. In this study, variegated WC1 gene expression within subpopulations and differences in signaling and cell activation due to endodomain sequences are described. The endodomains designated types I to III differ by a 15- or 18-aa insert in type II and an additional 80 aa containing an additional eight tyrosines for type III. Anti-WC1 mAbs enhanced cell proliferation of γδ T cells when cross-linked with the TCR regardless of the endodomain sequences. Chimeric molecules of human CD4 ectodomain with WC1 endodomains transfected into Jurkat cells showed that the tyrosine phosphorylation of the type II was the same as that of the previously reported archetypal sequence (type I) with only Y_{24}EEL phosphorylated, whereas for type III only Y_{199}DDV and Y_{56}TGD were phosphorylated despite conservation of the Y_{24}EEL/Y_{24}QEI and Y_{199}DDV/I tyrosine motifs among the three types. Time to maximal phosphorylation was more rapid with type III endodomains and sustained longer. Differences in tyrosine phosphorylation were associated with differences in function in that cross-linking of type III chimeras with TCR resulted in significantly greater IL-2 production. Identification of differences in the signal transduction through the endodomains of WC1 contributes to understanding the functional role of the WC1 coreceptors in the γδ T cell responses. ***The Journal of Immunology*****, 2014, 193: 379–390.**

Multigene families of pathogen recognition receptors (PRR) recognize pathogen-associated molecular patterns from a diverse array of bacteria, viruses, and protozoa (1). TLRs are exemplars of the critical role played by PRRs in the immune responses of mammals, *Drosophila*, and even plants (2). Their discovery has necessitated a re-evaluation of the importance of multigene families of conserved immune receptors, because, even though such receptors do not display the combinatorial diversity of the TCR and BCR, they can effectively discriminate between self and nonself in an immediate rapid fashion (3). Whereas PRRs are most frequently associated with the study of innate immunity, they are also involved in activating nonconventional T cells, including γδ T cells (1) and CD1d-restricted αβ T cells (4). Evidence suggests these cells are fully activated when their clonal TCR is engaged together with PRRs (4). This observation is consistent with γδ T cells' role as bridges between innate immune system cells (e.g., macrophages) that rely solely on PRRs for pathogen recognition and conventional αβ $CD4^+$ and $CD8^+$ T cells that use their clonal TCR as the principal recognition structure for Ag (5). Understanding how to activate nonconventional T cells is particularly important because they are involved in protective immunity against pathogens that require cellular immunity—the same pathogens to which it has proven difficult to develop vaccines. Because nonconventional γδ T cells can react with nonprotein Ags and direct adaptive immune responses, engaging these cells can reasonably be expected to optimize vaccination strategies. However, how to engage them is an unresolved fundamental question of practical importance.

Multiple members of the ancient scavenger receptor cysteine-rich (SRCR) superfamily are involved in modulating immune responses, including the γδ T cell coreceptors known as WC1 or T19, which are the subject of this research [reviewed in (6)]. Other SRCR members with this function include the following that directly bind bacterial or fungal components: SCARA5 (6), MARCO (7, 8), Spα (9), CD6 (10), CD163A (11), DMBT1 (12, 13), and CD5 (14). Of the SRCR superfamily members, WC1 molecules have the highest percentage identity with the CD163 family, which includes CD163A, CD163b, and CD163c-α in humans. That is, although CD163 family members have unique SRCR domains, they also share several signature conserved SRCR domains [b, c, d, e, and d′ (15)] with WC1. CD163c-α and WC1 molecules are particularly similar and hybrid assortments of CD163c-α–unique SRCR domains and WC1-unique SRCR domains occur in platypus and chicken molecules (15). CD163c-α and WC1 endodomains also share an intracellular YEEI/L motif required for WC1-mediated γδ T cell activation (15–17). SCART2, one of the two murine CD163c-α genes, is expressed on murine γδ T cells and may serve functions equivalent to WC1 in ruminants (18).

*Department of Veterinary and Animal Sciences, University of Massachusetts, Amherst, MA 01003; and †Program in Molecular and Cellular Biology, University of Massachusetts, Amherst, MA 01003

[1]Current address: Cornell Medical College, New York, NY.

Received for publication February 7, 2014. Accepted for publication April 30, 2014.

This work was supported by Agriculture and Food Research Initiative Competitive Grant 2011-67015-30736 and National Institutes of Health Grant R01 HD070056-01 from the National Institute of Food and Agriculture, U.S. Department of Agriculture–National Institutes of Health program titled Dual Purpose with Dual Benefit: Research in Biomedicine and Agriculture Using Agriculturally Important Domestic Species.

Address correspondence and reprint requests to Dr. Cynthia L. Baldwin and Dr. Janice C. Telfer, University of Massachusetts, Integrated Sciences Building, Amherst, MA 01003. E-mail addresses: cbaldwin@vasci.umass.edu (C.L.B.) and telfer@vasci.umass.edu (J.C.T.)

Abbreviations used in this article: PRR, pathogen recognition receptor; Q-PCR, quantitative PCR; SH2, Src homology 2; SRCR, scavenger receptor cysteine-rich; WT, wild-type.

www.jimmunol.org/cgi/doi/10.4049/jimmunol.1400168

We have shown that there are 13 WC1 molecules, whose expression defines subsets of bovine γδ T cells (16, 19). The expression of the WC1 genes defines the subset of γδ T cells that respond to the spirochete bacteria *Leptospira*, and they also contribute to the ability of T cells to do so (20, 21). That is, we have shown that γδ T cells activated by the bacterial pathogen *Leptospira* serovar Hardjo in recall responses are restricted to γδ T cell subsets within the serologically defined WC1.1$^+$ subset, and reduction of WC1 gene products in the WC1.1$^+$ subset reduces the γδ T cell response to the spirochete (20, 21). In contrast, a different subset of γδ T cells expressing WC1 proteins within the serologically defined WC1.2$^+$ group is implicated in the γδ T cell response to the rickettsia *Anaplasma* (22). WC1.1$^+$ and WC1.2$^+$ γδ T cells have a similar repertoire in their γδ-TCR usage in that both only use TCR-γ genes in the Cγ5-containing cassette, but all TCR-δ genes (23); thus, the functional differences between WC1.1$^+$ and WC1.2$^+$ T cells are likely to be derived from differential WC1 gene transcription (22–24). WC1 stimulation can augment suboptimal responses generated through the TCR/CD3 complex in a tyrosine phosphorylation-dependent manner; however, γδ T cells are not activated by Ab cross-linking of the WC1 coreceptors alone (17, 25). Although the γδ-TCR does not bind to Ag presentation molecules plus peptide Ag as the αβ-TCR does, the γδ-TCR/CD3 complex does require ligation by constrained molecules with sufficient affinity to signal (26). WC1 localizes to plasma membrane lipid rafts, which is required for TCR/CD3 signaling (20, 27). These observations led to the hypothesis that the WC1 molecules act as a hybrid PPR and coreceptor for the γδ-TCR, with WC1 and the γδ-TCR being cross-linked by the same or proximal ligands constrained on a surface such as a bacterial cell wall or cell membrane.

The 13 genes coding for the WC1 coreceptor family in cattle can be classified into three types based on unique exon–intron structures in their cytoplasmic domains (16). Endodomains of type I genes (*WC1-1*, *WC1-2*, *WC1-3*, *WC1-4*, *WC1-5*, *WC1-6*, *WC1-7*, *WC1-8*, and *WC1-13*), type II genes (*WC1-9*, *WC1-10*, and *WC1-12*), and type III gene (*WC1-11*) are coded by four, five, or six exons, respectively (16). Both type I and type II WC1 endodomains have five putative src family tyrosine kinase consensus phosphorylation sites (16, 17). The type III endodomain (*WC1-11*) has eight possible tyrosine kinase phosphorylation sites (16). We have shown that phosphorylation of the second tyrosine in the type I endodomains (Y_{24}EEL) is required for WC1-mediated potentiation of T cell activation through the TCR (17). That is, the extra 15 aa in type II (i.e., *WC1-9*) endodomains and additional tyrosine kinase phosphorylation motifs within the unique portion of the bovine type III (i.e., *WC1-11*) cytoplasmic region could result in functional outcomes that differ from those when WC1 molecules with type I endodomains are cross-linked with TCR/CD3.

In this study, the distribution of the WC1 gene products among the subpopulations of γδ T cells defined by mAbs and the effect the endodomain differences have on signaling and cell activation were evaluated, using both ex vivo γδ T cells as well as chimeric molecules composed of WC1 endodomains and human CD4 ectodomains expressed in adherent and Jurkat T cell lines.

Materials and Methods

Animals and lymphocytes

Blood was obtained from Holstein cattle between 1 and 2 y of age via jugular venipuncture and collected into heparin, under protocols approved by the University of Massachusetts Amherst Institutional Animal Care and Use Committee. PBMC were isolated from blood via density-gradient centrifugation over Ficoll-Paque (LKB-Pharmacia Biotechnology, Piscataway, NJ) by standard techniques.

RNA isolation

RNA was isolated from either ex vivo PBMC, CD4$^+$, or subpopulations of WC1$^+$ cells sorted via magnetic beads or flow cytometry to >90% purity, using TRIzol (Invitrogen Life Technologies, Carlsbad, CA), according to the manufacturer's instructions. Total RNA was subjected to DNase (Promega, Madison, WI) digestion and then used for cDNA synthesis using a commercial reverse-transcriptase kit (Promega).

Analysis of WC1 expression in PBMC

For amplifying the transcripts coding for domain 1 ["a" pattern as defined by Sarrias et al., reviewed in (6)] of each of the 13 WC1 genes, real-time quantitative PCR (Q-PCR) amplification and analysis were performed using a Stratagene Mx3005P instruments with software version 4.01 (Stratagene, La Jolla, CA). Primers were as described previously (19). For quantification, standard curves for each of 13 WC1 genes were constructed by using plasmids containing each WC1 domain 1 sequence as templates with WC1 gene-specific primer pairs in Q-PCR. The GenBank accession numbers of the sequence used for designing the primers in this experiment have been described previously (19). The Q-PCR amplification mixture (25 μl) was as follows: 20 ng template DNA, 12.5 μl concentration of premixed reagent including Takara Ex Taq HS and SYBR Green I (TAKARA, Pittsburgh, PA), 0.5 μl ROX reference dye, and 1 μl forward and reverse primers to a final concentration of 0.5 μM each. Real-time PCR amplification was conducted for 35 cycles, each cycle consisting of 95°C for 5 s, 58°C for 20 s (with a single fluorescence measurement taken at the end of the annealing step), and 72°C for 20 s. Cycle threshold values were converted into zmol of WC1 transcripts using standard curves constructed from Q-PCR done with a defined amount of WC1 cDNA plasmid template titrated over a range of concentrations, as described (21). Q-PCR products were gel purified and cloned into the pCR2.1 vector (Invitrogen Life Technologies), according to the manufacturer's protocol for sequencing. Sequencing was performed commercially (Genewiz, South Plainfield, NJ) to verify amplicons. Multiple sequence alignments were performed using Clustalw2 (http://www.ebi.ac.uk/Tools/clustalw2/index.html website) (28) and the default parameters, but manually optimized when necessary, and were visualized using Bioedit version 7.0.5.3 (29). Significant differences of $p < 0.05$ were calculated using a one-way ANOVA with Bonferroni posttest, Prism 5, GraphPad.

Indirect immunofluorescence and cell proliferation

Cells were cultured for 1 or 3 d depending upon the assay. In some experiments, cells were labeled with eFluor 670 proliferation dye (eBioscience) to assess cell division. Cellular proliferation was analyzed by eFluor 670 proliferation dye dilution by flow cytometry. Cells were stained by indirect immunofluorescence for surface markers using the mAb, as follows: BAG25A (VMRD, Pullman, WA) for WC1.1; CACTB32A (VMRD) for WC1.2; CACT21A (VMRD) for WC1.3; IL-A29 and CC15, which are pan specific for all WC1 molecules (Serotec, Oxford, U.K.); GB21A (VMRD) for δ-TCR; and IL-A12 for CD4 (20, 30–32). Secondary Abs used for indirect staining were isotype-specific polyclonal goat anti-mouse Ig conjugated with PE or FITC (Southern Biotechnology Associates, Birmingham, AL). In staining procedures that used secondary Abs, unrelated isotype-matched primary mAbs with matching secondary Abs were used as negative controls (Southern Biotechnology Associates and BD Biosciences, San Jose, CA).

Magnetic bead and flow cytometric cell sorting

For magnetic bead cell sorting, PBMC were stained for surface markers at 4°C for 20 min in PBS with 2 mM EDTA and 0.5% BSA. The primary mAbs for WC1$^+$ cells described above were used for positive sorting. Cells were then incubated with goat anti-mouse IgG-conjugated or IgM-conjugated magnetic microbeads (Miltenyi Biotec, Auburn, CA) at 4°C for 20 min. After washing twice, cells were applied to the column following the manufacturer's instructions. The purity of collected fractions was assessed by flow cytometry and analyzed using FlowJo (Tree Star, Ashland, OR). For flow cytometric cell sorting, PBMC were stained with mAbs described above and sorted using a FACSAria (BD Biosciences).

Constructs and mutagenesis

To generate fusion proteins consisting of the ectodomain of human CD4 with the transmembrane domain and endodomains of *WC1-9* and *WC1-11*, the *WC1-9* and *WC1-11* transmembrane domains were amplified using the primer pair (WC1-9-*trans*-for 5′- CCACCCCTAGGCCAACCTCAAATCCTCTCTCT-3′ and WC1-9-*trans*-rev 5′- GGCTCTGCGCTCTGCTCTCC-3′) and the primer pair (WC1-11-*trans*-for 5′- CCACCCCTAGGTGCTCTG-

CTCCAGACCCT-3′ and WC1-11-*trans*-rev 5′- CTCTTGGTGCTCTGCTCTCC-3′), respectively, from an identified clone (16), and then integrated into each WC1 wild-type (WT) or mutant endodomain by overlapping PCR using primer pair (WC1-9-intrafor 5′-GAGGATCCAGCTGCTCAGACGGAGAGCAGAG-3′ and WC1-9-intrarev 5′-GACTCGAGTCATGAGAAAGTCATTGGGG-3′) and primer pair (WC1-11-intrafor 5′-GAGGATCCAGCTACACAGATGGAGAGCAGAG-3′ and WC1-11-intrarev 5′- GACTCGAGCTACATGGTGCTAAG-3′), respectively. The constructs and tyrosine mutants were generated as described previously (17). All of the DNA constructs mentioned above have been commercially sequenced (Genewiz) at least twice to validate sequence identity and to confirm the open reading frame. Nucleotide sequences were aligned and analyzed using BioEdit version 7.0.5.3 (29), and multiple sequence alignments were performed using ClustalW2 (33) and the default parameters.

Transfection of mammalian cells

Transfection of HEK-293 cells (American Type Culture Collection) was performed using Fugene HD (Roche, Palo Alto, CA), following the manufacturer's instructions. The ratio of DNA to Fugene HD was maintained at 1:3 (μg:μL). Two days after transfection, cells were harvested and brought into single-cell suspension in PBS supplemented with 5 mM EDTA. Cell surface expression of CD4/WC1 was analyzed by flow cytometry using direct immunofluorescence of FITC-conjugated mouse anti-human CD4 mAb (BD Biosciences).

Cell membrane extraction

HEK-293T cells transfected with CD4/WC1 constructs were harvested, resuspended in hypotonic extraction buffer (10 mM Tris-HCl [pH 7.4], 0.2 mM $MgCl_2$) containing 1 mM PMSF and 1 mM sodium orthovanadate (4×10^6 cells/ml) and incubated on ice for 10 min, followed by homogenization on ice. Lysates were combined with an equal volume of sucrose buffer (0.5 M sucrose, 2 mM EDTA) and centrifuged at 5000 × *g* for 10 min. The pellets were rehomogenized in sucrose extraction buffer (0.25 M sucrose, 1.0 mM EDTA, 10 mM Tris-HCl [pH 7.4]) and centrifuged at 5000 × *g* for 10 min. Supernatants from these two centrifugations were combined and centrifuged at 47,800 × *g* at 4°C for 30 min. Pellets were solubilized in 0.5% Triton-X lysis buffer (0.5% Triton-X, 50 mM Tris-HCl [pH 7.5], 150 mM NaCl) containing phosphatase inhibitor (Pierce, Rockford, IL) and protease inhibitor cocktails (Roche). Protein concentration was estimated by Bradford assay (Bio-Rad, Hercules, CA). Sixty micrograms of each protein per sample was resolved on 10% SDS-PAGE.

Stable expression of CD4/WC1 constructs in Jurkat T cells

The CD4/WC1 chimeric protein was subcloned into the NheI–ClaI site of pLEIGW from pBK-CMV, as described (17). Lentiviral supernatants were harvested 48 and 72 h after transfecting HEK-293 cells with a mixture of 1 μg pLEIGW, 0.25 μg pCMV-VSV-G, 0.75 μg pCMV△8.9, and 6 μL FuGeneHD. Lentiviral supernatants with 10 μg/ml Lipofectamine (Invitrogen Life Technologies) were added 16 h after Jurkat cells (2×10^5 cells/well) were seeded into six-well plates and were left for 48 h until cells were analyzed by flow cytometry. GFP^+ cells were enriched to >90% on the cell sorter and maintained in RPMI 1640 supplemented with 10% heat-inactivated FBS at 37°C with 5% CO_2.

Immunoblotting

Samples were transferred to polyvinylidene difluoride membranes (GE Health Care, Piscataway, NJ) and were preblocked in TBST containing 5% nonfat milk, except for experiments using anti-phosphotyrosine Ab, for which 5% BSA was used, for 1 h at room temperature. Membranes were then incubated with appropriate Abs in TBST containing 1% nonfat milk or BSA at room temperature for 1.5 h, following which they were washed twice for 10 min in TBST. They were then incubated with HRP-conjugated secondary Abs in TBST containing 1% nonfat milk or BSA at room temperature for 1 h. Membranes were washed at least three times before development with ECL Western blotting detection reagents (GE Health Care). In some experiments, membranes were stripped by incubating in buffer (10 μM 2-ME, 2% SDS, 62.5 mM Tris-HCl [pH 6.7]) for at least 30 min at 60°C and reprobed with other Abs. PhotoShop (Adobe, San Jose, CA) was used to quantitate band signals. Mouse anti-phosphotyrosine mAb 4G10 (Upstate, Billerica, MA) was used for phosphotyrosine blotting; rabbit anti-human CD4 Ab (H-370; Santa Cruz Biotech) was used for detecting CD4/WC1 chimeric proteins. HRP-conjugated goat anti-rabbit IgG (GE Health Care) or HRP-conjugated protein A (Upstate) was used as the secondary reagent. Signal was measured, and the ratio of anti-phosphotyrosine signal to anti-CD4 signal (area density ratio) was calculated.

Cytokine ELISA

Culture supernatants from activated cells were harvested and used to analyze different cytokines by ELISA. For stimulation of Jurkat cells with plate-bound Abs, anti-CD4 (5 μg/ml; OKT4; eBioscience, San Diego, CA) and anti-CD3 (2 μg/ml; UCHT1; eBioscience) were incubated in 96-well plates at 4°C for 12 h and rinsed with PBS before use. Jurkat cells (1×10^5 cells/ml, 200 μl/well) were incubated at 37°C for 48 h in precoated wells or with PMA and ionomycin (50 ng/ml of each). OptEIA Human IL-2 ELISA kit (BD Biosciences) was used following the manufacturer's instructions for detecting IL-2 production.

Results

Subpopulations of $WC1^+$ γδ T cells defined by expression of WC1 molecules with different types of WC1 endodomains

We have shown there are 13 WC1 genes in cattle conserved among breeds and individuals (16, 19). Although we have shown that WC1 molecules are an important contributor to the γδ T cell response to the spirochete bacteria *Leptospira* (21), the sequencing of transcripts and genome annotation showed that three different endodomain sequences existed among the 13 WC1 genes (Fig. 1) in addition to the two types of ectodomain structures. With regard to the latter, it has been hypothesized that the WC1 molecules with six SRCR domains are the more ancient (34) and gave rise to the 11 SRCR forms that have a duplication of the b-c-d-e-d domains (16, 19). In this study, we investigate how the differences in the cytoplasmic tail sequences affect signaling, and how they are distributed among cell populations because this was unknown.

To begin to address this, we referred to the observation that bovine γδ T cells are divided into subsets by mAbs reactive with the ectodomains of WC1 molecules (31, 32, 35). These serologically defined WC1 molecules were designated as WC1.1, WC1.2, and WC1.3 decades ago with WC1.1 and WC1.2 epitope-bearing WC1 molecules expressed on two mostly nonoverlapping subsets of bovine γδ T cells and the WC1.3 epitope expressed on a small subpopulation within the $WC1.1^+$ population (31, 32). Whereas we have mapped the molecules and SRCR domains reactive with the panel of mAbs (Table I, Fig. 2A) (35), not all WC1 molecules react with one or more of the panel of mAbs. Thus, how the WC1 family members are distributed among the serologically defined subpopulations was unknown. Thus, four serologically defined subpopulations were isolated by flow cytometric sorting (Fig. 2B), and their WC1 transcripts were evaluated by quantitative RT-PCR.

Because the N-terminal WC1 domain (e.g., domain 1) contains the most variability among WC1 genes (16), this domain was targeted for WC1 gene-specific transcript analysis (19). The WC1 gene-specific primer sets uniquely amplified 1 of the 13 WC1 SRCR domain 1 sequences under the experimental conditions used. The $WC1.1^+$ γδ T cell subpopulation was found to express significant levels of *WC1-2*, *WC1-3*, *WC1-6*, *WC1-8*, *WC1-10*, *WC1-11*, and *WC1-13* transcripts and thus contained WC1 molecules with type I, II, and III endodomains (Fig. 2C). These results are consistent with our previous observations that anti-WC1.1 mAb BAG25A recognizes domain 1 of *WC1-1*, *WC1-2*, *WC1-3*, *WC1-5*, and *WC1-11*, whereas anti-WC1.2 mAb CACTB32A recognizes domain 1 of WC1-4 and *WC1-9* (35). However, *WC1-6*, *WC1-8*, *WC1-10*, *WC1-12*, and *WC1-13* transcripts were also present at significant levels in $WC1.1^+$ T cells (Table II), although their gene products are not recognized by the anti-WC1.1 subpopulation-specific BAG25A mAb (Table I) (35).

The sorted $WC1.2^+$ T cell subpopulation had significant expression of *WC1-4*, *WC1-7*, and *WC1-9* transcripts (Fig. 2C) and thus likely has WC1 molecules with type I and II endodomains. Whereas WC1-4 and WC1-9 are both recognized by anti-WC1.2 mAb CACTB32A (Table I), *WC1-7* transcripts were also found

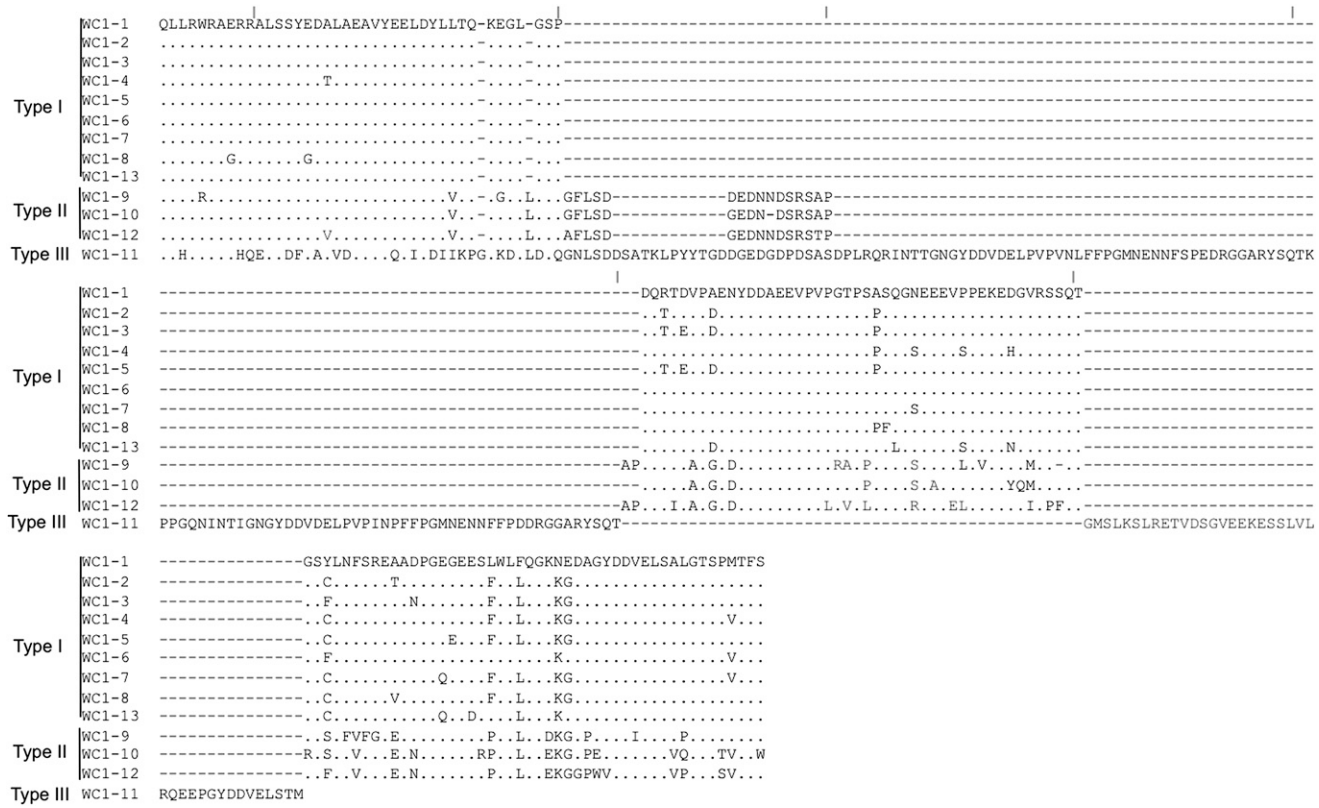

FIGURE 1. Alignments of 13 WC1 endodomain-deduced amino acid sequences. WC1 endodomain-deduced amino acid sequences were aligned with ClustalW2 using the default parameters and visualized with JalView. Analysis includes all nonredundant genomic sequences as described previously (16, 19). Identity is indicated by periods (.) and gaps by hyphens (-). The small vertical lines above the sequence indicate approximate exon boundaries that may occur within the codon for some amino acids.

in the sorted WC1.2$^+$ T cells but are not recognized by the CACTB32A (Table II).

The WC1.3$^+$ subpopulation (CACT21A$^+$) had predominantly *WC1-8* transcripts, but also *WC1-3* transcripts (Fig. 2C), even though CACT21A mAb only reacts with WC1-8 SRCR domain 1 (Fig. 2A). WC1.3$^+$ T cells are a subpopulation within the WC1.1$^+$ T cell population defined by BAG25A mAb; thus, the presence of WC1-3 accounts for the reactivity with BAG25A mAb because WC1-8 was not recognized by BAG25A mAb (Fig. 2A). From this, we can conclude that the mAb CACT21A defines cells that coexpress WC1-8 and WC1-3 type I endodomain molecules. The WC1.1$^+$/WC1.2$^+$ double-positive population had significant levels of *WC1-1* and *WC1-5* transcripts whose gene products are both reactive with the WC1.1 mAb BAG25A, whereas WC1-1 is also recognized by WC1.2 mAb CACTB32A (Table I). Both of these WC1 molecules have type I endodomains.

Table I. mAb reactivity with various WC1 molecules

SRCR Domain 1 from	mAb BAG25A (anti-WC1.1)	mAb CACT21A (anti-WC1.3)	mAb CACT32A (anti-WC1.2)
WC1-1	+		+
WC1-2	+		
WC1-3	+		
WC1-4			+
WC1-5	+		
WC1-6			
WC1-7			
WC1-8		+	
WC1-9			+
WC1-10			
WC1-11	+		
WC1-12			
WC1-13			

The first domain ("a" pattern) was expressed from each of these WC1 genes and evaluated for reactivity with the mAbs designated either here or previously (Fig. 2A) (35). The designations WC1.1, WC1.2, and WC1.3 are serological designations established previously (31, 32, 35). +, positive reactivity with the mAb.

Proliferation of ex vivo primary bovine γδ T cell subpopulations induced by Abs that react with WC1 with various endodomains

The three anti-WC1 mAbs (WC1.1 BAG25A, WC1.2 CACTB32A, and WC1.3 CACT21A) react with different combinations of WC1 molecular types (Table II). Because subtle sequence variations between endodomains could affect intracellular signaling, we evaluated the proliferation of ex vivo primary bovine γδ T cells in cross-linking assays with these subpopulation-defining anti-WC1 mAbs plus anti-TCR mAb. The proliferation of bovine γδ T cells stimulated by cross-linking of pan-reactive anti-WC1 mAb IL-A29 in combination with the anti-TCR mAb was used as a positive control because IL-A29, in conjunction with anti-TCR mAb, has been shown to activate γδ T cells by our laboratory (25) and reacts with the majority of WC1$^+$ cells.

It was noticeable that the enhancement of bovine γδ T cell proliferation varied among the four different cross-linking Abs, but this was consistent with the proportions of cells in PBMC with which the anti-WC1 mAbs react (data not shown). We gated each WC1$^+$ γδ T cell subpopulation to rule out possible effects of differences in the proportional representation of each subpopulation within PBMC, and a representative of the gating strategy for dividing cells in various WC1$^+$ γδ T cell subpopulations is shown in Fig. 3A. The proliferation enhancement of each subpopulation was then evaluated (Fig. 3B). We also note in this work, as we

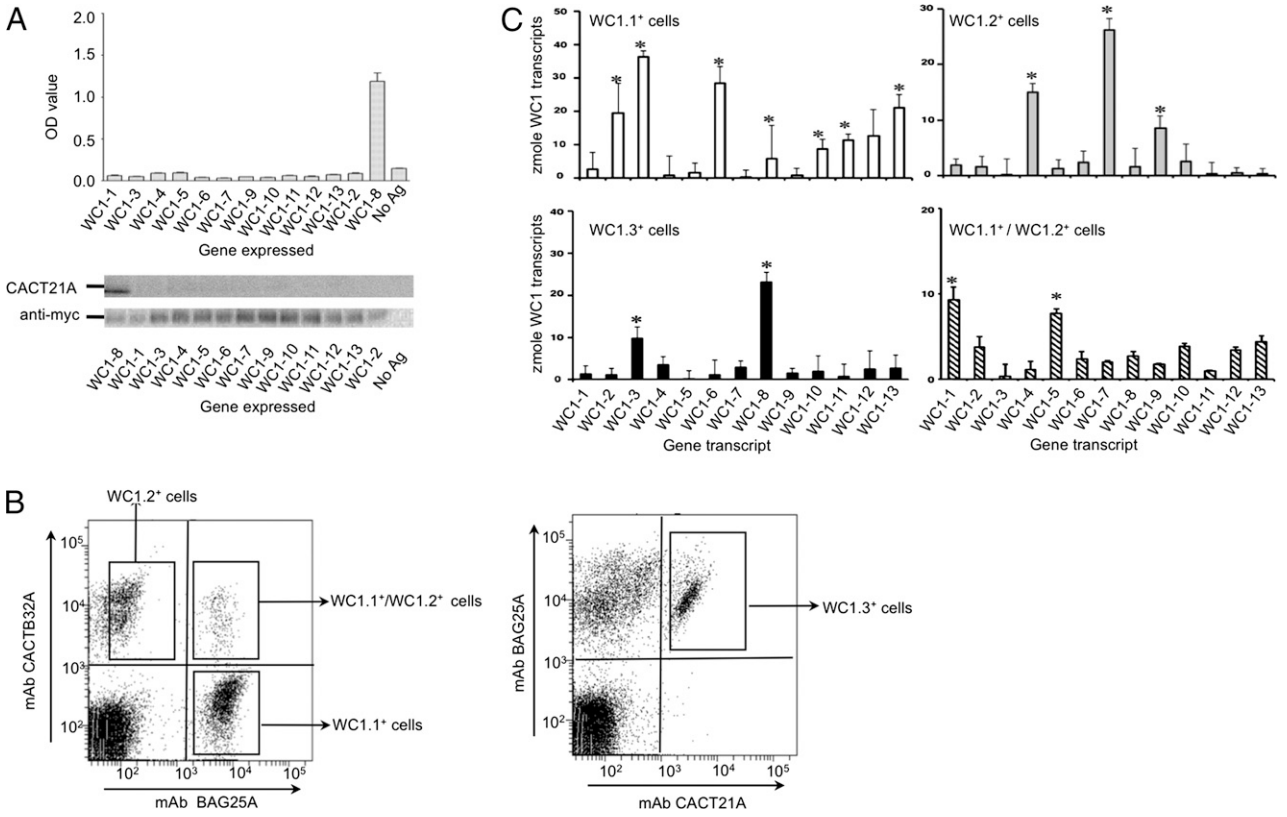

FIGURE 2. Subpopulations of WC1$^+$ γδ T cells defined by expression of WC1 molecules with different types of WC1 endodomains. (**A**) Ab CACT21A was evaluated for reactivity against the myc-tagged domain 1 proteins of 13 WC1 molecules in ELISA and immunoblotting. Negative controls included no Ag (no Ag). The OD values represent the mean ± SEM for three independent experiments. (**B**) PBMC stained with anti-WC1.1 mAb BAG25A, anti-WC1.2 mAb CACTB32A, and anti-WC1.3 mAb CACT21A were analyzed via flow cytometry (100,000 events). The *left panel* shows the PBMC staining with mAb BAG25A and mAb CACTB32A. The *right panel* shows the PBMC staining with mAb BAG25A and mAb CACT21A. The gated populations are indicated in the figure. (**C**) Zmol of WC1 gene transcripts present in the WC1.1$^+$/WC1.2$^-$ subpopulation (BAG25A$^+$/CACTB32A$^-$, empty bars), the WC1.1$^-$/WC1.2$^+$ subpopulation (BAG25A$^-$/CACTB32A$^+$, gray bars), the WC1.3 subpopulation (mAb CACT21A$^+$, black bars), and the WC1.1$^+$/WC1.2$^+$ subpopulation (BAG25A$^+$/CACTB32A$^+$ striped bars). Mean values ± SE for $n = 5$ replicates from two independent experiments are represented, and significant differences ($p < 0.05$, one-way ANOVA with Bonferroni posttest, Prism 5, GraphPad) between any 2 of 13 WC1 transcripts within a subpopulation are indicated by asterisks.

have previously published, the WC1.2$^+$ cells are particularly susceptible to Con A activation (20).

BAG25A mAb reacts with type I and III WC1 molecules, whereas CACTB32A mAb reacts with type I and type II WC1 molecules and CACT21A mAb only recognizes type I WC1 molecules and all enhanced proliferation when compared with the cells stimulated by anti-TCR alone (Fig. 3B, 3C). Cross-linking with anti-TCR mAb and anti-WC1 IL-A29 mAb induced the greatest levels of proliferation for each of the subpopulations, presumably reflecting a dose effect in that IL-A29 reacts broadly with WC1 molecules with type I, II, and III endodomains. However, there are a number of limitations to these experiments. The number of different WC1 gene products expressed by an individual cell is unknown except for the WC1.3$^+$ cells. (These cells are double positive for the anti–WC1-8 mAb CACTB21A and anti–WC1-3 mAb BAG25A, and cDNA analysis indicates these

Table II. WC1$^+$ γδ T cell subpopulations defined serologically

Population Designation (mAb Used To Define)	Type of Endodomain	WC1 Transcripts Associated with the Serologically Defined Population	
		These Genes Code for Proteins Reactive with the Defining mAb	These Genes Code for Proteins Not Reactive with the Defining mAb
WC1.1$^+$/WC1.2$^-$ (mAb BAG25A)	I	WC1-2, WC1-3	WC1-6, WC1-8, WC1-13
	II	—	WC1-10, WC1-12
	III	WC1-11	—
WC1.2$^+$/WC1.1$^-$ (mAb CACTB32A)	I	WC1-4	WC1-7
	II	WC1-9	—
	III	—	—
WC1.1$^+$/WC1.2$^+$ (mAb BAG25A and mAb CACTB32)	I	WC1-1, WC1-5	—
	II	—	—
	III	—	—
WC1.3$^+$ (mAb CACT21A)	I	WC1-8	WC1-3
	II	—	—
	III	—	—

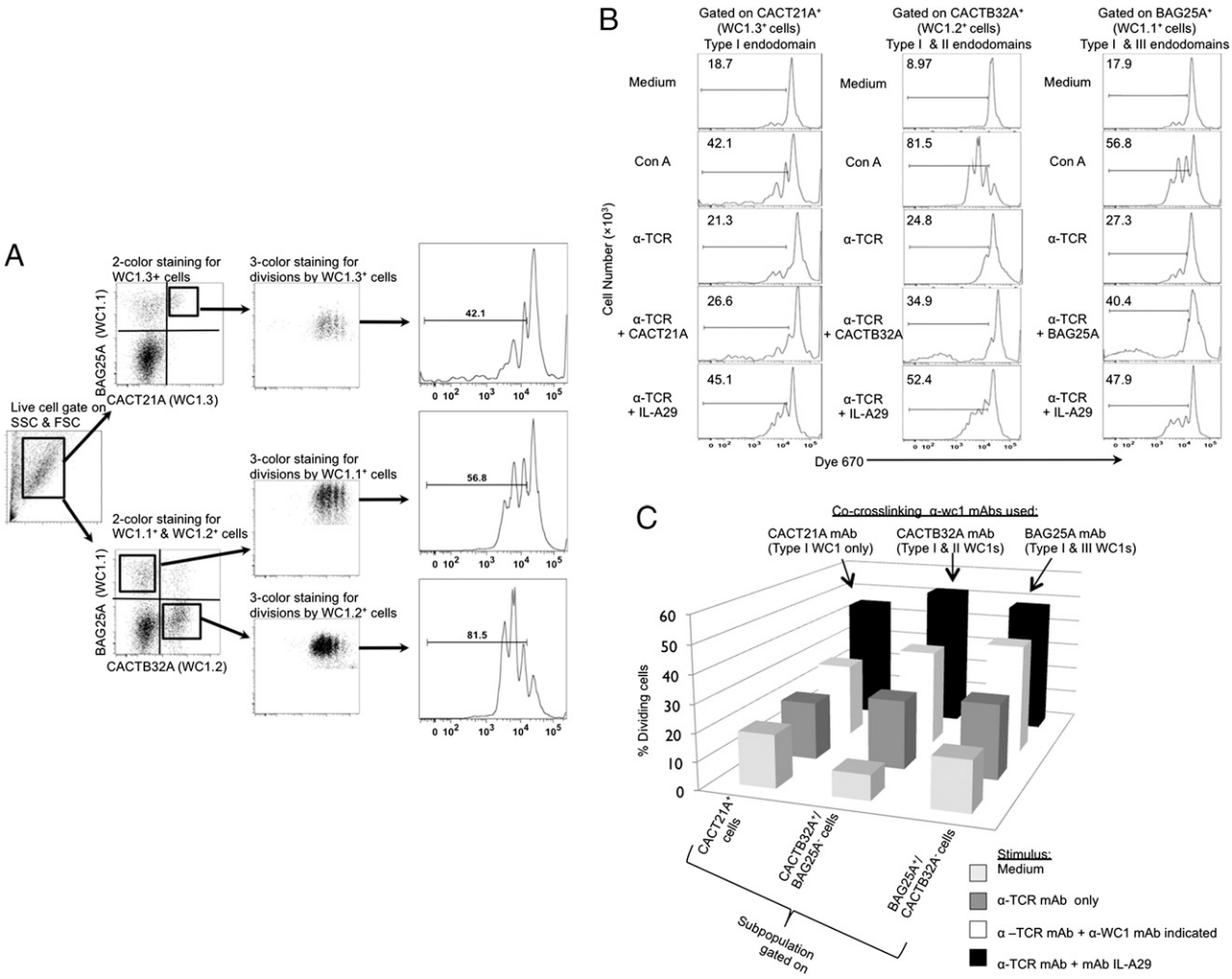

FIGURE 3. Proliferation of ex vivo primary bovine γδ T cell subpopulations induced by Abs that react with WC1 with various endodomains. (**A**) A representation of the gating strategy to determine dividing cells in the various subpopulations is shown using Dye670-loaded PBMC and culturing with Con A. (**B**) Dye670-PBMC were cultured for 3 d with medium only, plate-bound anti-TCR mAb (1 μg/ml) only, or plate bound anti-TCR (1 μg/ml) plus anti-WC1 mAb (anti-WC1.1 mAb BAG25A, 10 μg/ml; anti-WC1.2 mAb CACTB32A, 10 μg/ml; anti-WC1.3 mAb CACT21A, 10 μg/ml; or anti-pan $WC1^+$ mAb ILA29, 10 μg/ml). Cells were gated for viability and $WC1.1^+$ ($BAG25A^+$), $WC1.2^+$ ($CACTB32A^+$), and $WC1.3^+$ ($CACT21A^+$) subpopulations before plotting for Dye670 intensity. These results are representative of two experiments. (**C**) Summary of the proliferation of $WC1.1^+$ ($BAG25A^+$), $WC1.2^+$ ($CACTB32A^+$), and $WC1.3^+$ ($CACT21A^+$) subpopulations stimulated by Abs that react with WC1 gene products, as detailed in Table I.

are the only two genes transcribed.) Also, the different mAbs may not be equivalently good at stimulating proliferation even though in ELISA-binding studies using recombinant target proteins, anti-WC1.1 mAb BAG25A, anti-WC1.2 mAb CACTB32A, and anti-WC1.3 mAb CACT21A resulted in a similar OD (35) (Fig. 2A), suggesting comparable affinities. The number of WC1 molecules representing the various WC1 gene products on an individual cell is unknown, and finally we cannot account for the activation state of the individual γδ T cells within a subpopulation prior to the assay, even though all are ex vivo. Such differences may account for the fact that some γδ T cells do not divide in the assay period whereas others seem to divide a number of times (Fig. 3B). Thus, further molecular studies were done in defined system to compare signaling through the three different endodomains more precisely, that is, using recombinant molecules and transfection and transduction experiments described below.

Consensus src tyrosine kinase phosphorylation site motifs of WC1 endodomains are determined by sequence insertions

Previously, we investigated the role of tyrosine phosphorylation in type I endodomains (17). In this study, we extended that for type II and III endodomains using *WC1-9* as a representative of a type II endodomain with five tyrosines (Fig. 4A). All five tyrosines are conserved between the type I and II endodomains, with the first and second tyrosines falling into an ITAM-like motif (Y_{15}EDA X_5 Y_{24}EEL) and the other three tyrosine motifs being Y_{29}LLT, Y_{70}DDA, and Y_{138}DDV (Fig. 4A). Phosphorylation of the second tyrosine (Y_{24}EEL) in the type I WC1 endodomain is required for WC1 potentiation of T cell activation through the TCR (17), potentially providing a docking site for a Src homology 2 (SH2)–containing adaptor protein such as Shc (36). Although the type I and type II endodomains have five tyrosine motifs in common, it is possible that the extra 14 or 16 aa (GFLSDDEDNNDSRS[AP]) in type II endodomains could alter the cytoplasmic domain, resulting in signaling differences relative to the type I endodomains. The single type III endodomain (*WC1-11*) contains three of five tyrosines conserved with those in type I and type II endodomains. The remaining tyrosine motifs of type I/II (Y_{15}EDA and Y_{29}LLT) are changed to F_{15}EAA and D_{29}IIK in type III. Of the three conserved tyrosines, two tyrosine motifs in the type III endodomain diverge by 1–2 aa from that in the other endodomains, changing from Y_{24}EEL to Y_{24}QEI and from Y_{70}DDA to $Y_{70/138}$DDV while

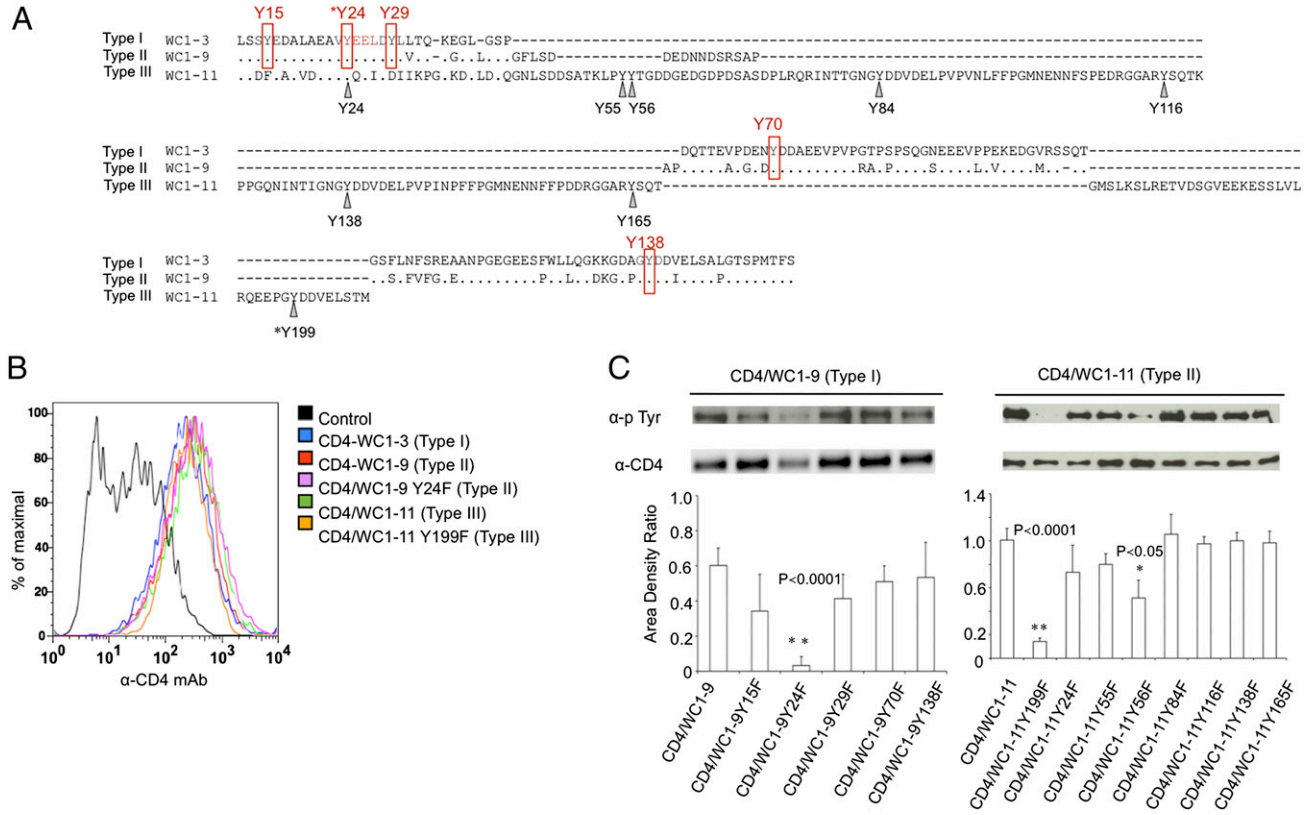

FIGURE 4. Tyrosine motifs of WC1 type I, II, and III endodomains. (**A**) Deduced amino acid sequence from transmembrane regions and intracytoplasmic tails of *WC1-9*, *WC1-11*, and the archetypal WC1 sequence (*WC1-3*) were aligned using ClustalW2 using the default parameters and refined manually. GenBank accession numbers (https://www.ncbi.nlm.nih.gov/genbank/) for amino acid sequences used for comparison are as follows: WC1-3 type I endodomain (archetypal WC1.1; X63723; *WC1-3*), WC1-9 type II endodomain (FJ031208; *WC1-9*), and WC1-11 type III endodomain (FJ031209; *WC1-11*). Identities are indicated by periods (.) and gaps by hyphens (-). The five tyrosines shared by WC1-3 and WC1-9 (rectangles) and the eight tyrosine residues in WC1-11 (arrowheads) are indicated. Amino acids are numbered from the beginning of the cytoplasmic tail. The tyrosine residues that were found to be the main targets of tyrosine kinases in this study were indicated by asterisks. (**B**) Jurkat cells were infected with lentivirus encoding CD4/WC1-3 WT, CD4/WC1-9 WT, CD4/WC1-9 Y24F (second tyrosine mutated to phenylalanine), CD4/WC1-11 WT, or CD4/WC1-11 Y199F (eighth tyrosine mutated to phenylalanine) individually. Empty lentiviral vector was used as a control. Transduced cells were enriched by flow cytometry based on their GFP expression and stained with PE-conjugated mouse anti-human CD4. (**C**) Cell membrane extracts of 293T cells transfected with 2 μg each of pBK-CMV CD4/WC1-9 and CD4/WC1-11 constructs were immunoblotted with anti-phosphotyrosine mAb 4G10. Membranes were stripped and reprobed with rabbit anti-human CD4 Ab to determine the amount of CD4/WC1 proteins expressed. The amount of phosphotyrosine signal was normalized to the amount of CD4/WC1 proteins detected by anti-CD4 Ab. The phosphorylation intensity of each chimeric protein was measured, and the ratio of anti-phosphotyrosine signal to anti-CD4 signal (area density ratio) was determined and represented as mean ± SD for three experiments. Significant differences between WT and mutant CD4/WC1, as determined by *t* test (one tailed), are marked by asterisks, and each corresponding *p* value is shown above the bar.

Y_{199}DDV in the type III endodomain is conserved with the unphosphorylated Y_{138}DDV in the type I endodomain. In addition, the WC1-11 type III endodomain contains another five unique tyrosines (Fig. 4A).

To determine which tyrosine residues contribute to the phosphorylation of the type II and III endodomains, chimeric proteins of the ectodomain of human CD4 with the WC1-9 and WC1-11 transmembrane domains and endodomains were constructed. From these, a series of endodomain mutants with each tyrosine substituted by phenylalanine individually were also generated. CD4/WC1-9, CD4/WC1-11 WT unmutated and mutant chimeric proteins were expressed on the surface of Jurkat T cells by lentiviral transduction and stable surface expression confirmed by staining with an anti-CD4 mAb (Fig. 4B). The phosphorylation level of WT WC1 endodomains and mutants expressed in 293T cells was evaluated by immunoblotting with anti-phosphotyrosine Ab normalized to the CD4-WC1 endodomain fusion protein (Fig. 4C). In previous studies, we evaluated phosphorylation of WC1 cytoplasmic domains and their mutants first as recombinant GST fusion proteins produced in bacteria and then as CD4-WC1 cytoplasmic domain fusion protein produced in 293T cells, which gave the same results. The 293T cells are readily transiently transfectable, unlike Jurkat T cells. Transient transfection allows for high throughput of plasmid constructs, with protein expressed at a high level. High-level protein expression is critical to increase the signal to noise ratio. We used membrane fractions to further decrease background.

As seen previously with type I endodomains, when the second tyrosine residue (Y_{24}) in WC1 type II (*WC1-9*) endodomain was mutated to phenylalanine, tyrosine phosphorylation was greatly reduced (17) (Fig. 4C). In contrast, the equivalent Y24F mutation in the WC1 type III (*WC1-11*) endodomain did not reduce tyrosine phosphorylation, indicating that Y24 in the type III endodomain is not phosphorylated (Fig. 4C). However, mutation of the last tyrosine in the WC1 type III (*WC1-11*) endodomain (Y199F, equivalent to Y138F in WC1 type I and II endodomains) virtually abrogated tyrosine phosphorylation of the fusion protein (Fig. 4C). Mutation of other tyrosine residues did not affect the phosphorylation of the WC1 type II endodomain (*WC1-9*), although mutation of the second unique tyrosine in the type III (*WC1-11* Y56F)

endodomain resulted in a decrease in tyrosine phosphorylation ranging from 20 to 40% in three experiments. Thus, the phosphorylation of tyrosines other than Y_{24} was only observed with the type III (*WC1-11*) endodomain, not with type II (*WC1-9*) endodomain or previously with the type I endodomain (17). The unphosphorylated Y_{24}QEI motif in the WC1 type III endodomain is minimally changed from the phosphorylated motif in WC1 type I and II endodomains and should still be able to be phosphorylated. The Y_{199}DDV motif phosphorylated in the WC1 type III endodomain is the same as the unphosphorylated Y_{138}DDV motif in WC1 type I and II domains. Taken together, these results suggest that the longer length of the WC1 type III endodomains alters the accessibility of the tyrosines to the kinase.

Kinetics of optimal tyrosine phosphorylation varies depending upon the WC1 endodomain expressed

A previous study showed that tyrosine phosphorylation of the Y_{24}EEL motif in type I WC1 endodomain is required for WC1 potentiation of T cell activation through the TCR (17). To study whether phosphorylation of Y_{24}EEL in type II (*WC1-9*) or Y_{199}DDV in type III (*WC1-11*) endodomains has the same potential to act as costimulatory receptors for TCR signaling as the type I endodomain, CD4/WC1-3 (type I), CD4/WC1-9 (type II), and CD4/WC1-11 (type III) chimeric proteins were expressed in Jurkat T cells. Because previously and in this study we showed that the endogenous level of CD4 in Jurkat T cells was >20-fold lower than CD4/WC1 chimeric protein (17) (Fig. 4B), anti-CD4 mAb cross-linking of Jurkat T cells bearing CD4/WC1 chimeric molecules would be expected to result in the majority of the cross-linking to be the CD4/WC1 chimeric proteins rather than the endogenous CD4.

A preliminary cross-linking assay was performed with anti-CD4 Ab in the presence or absence of anti-CD3 Ab. Whereas the WT CD4/WC1-3 (type I) and CD4/WC1-9 (type II) endodomains showed phosphorylation when cross-linked regardless of whether anti-CD3 Abs were included, when the second tyrosine (Y24) was mutated to phenylalanine no phosphorylation was seen (data not shown). Similarly, WT but not the CD4/WC1-11 Y199F mutant showed phosphorylation after cross-linking (data not shown). It further confirmed in Jurkat T cells that the membrane-proximal Y_{24}EEL is the only target of tyrosine kinases in type I and type II WC1 endodomains, whereas in the type III WC1 endodomain, tyrosine kinases instead target Y_{199}DDV, the last tyrosine in type III WC1 endodomain.

Kinetic analyses were then conducted for the chimeric molecules containing the type II and III endodomains (Fig. 5). Using WT endodomains, Ab-mediated cross-linking of WC1 with the TCR initially resulted in a more profound increase in tyrosine phosphorylation compared with cross-linking with anti-WC1 mAb alone (Fig. 5), which is consistent with our previous observation for type I endodomain (17). This observation indicates that proximal TCR engagement is required for the optimal tyrosine phosphorylation of all three types of WC1 endodomains. In addition, the time-dependent increase in tyrosine phosphorylation was seen with all three types of WC1 endodomains (Fig. 5), but the kinetics of tyrosine phosphorylation and the maximal levels reached differed among the three types of WC1 endodomains (Fig. 5). The maximal level occurred earlier when cross-linking WC1 alone (at ~0.5 min) with type I and II endodomains than for the type III (at ~1 min) (Fig. 5). When we cross-linked WC1 and TCR, the kinetics of tyrosine phosphorylation was also similar between WT CD4/WC1-3 (type I) and CD4/WC1-9 (type II) in Jurkat T cells, with maximal levels reached by ~1 min, followed by a gradual decrease (Fig. 5). However, cross-linking of WT CD4/WC1-11 (type III) and TCR resulted in faster tyrosine phosphorylation (maximal level reached at ~0.5 min) than the tyrosine phosphorylation resulting from cross-linking WT CD4/WC1-3 (type I) and CD4/WC1-9 (type II) with the TCR (Fig. 5).

The enhancement of IL-2 production varies among Jurkat T cells expressing three different types of WC1 endodomains

Next, we tested whether phosphorylation of Y_{24}EEL in type II (*WC1-9*) WC1 endodomains was equivalent to phosphorylation of Y_{24}EEL in type I WC1 endodomains and whether phosphorylation of Y_{199}DDV in the type III (*WC1-11*) WC1 endodomain could compensate for the nonphosphorylation of Y_{24}QEI. A comparison of IL-2 production stimulated by PMA, plus ionomycin treatment of populations of Jurkat T cells expressing CD4/WC1-3WT, CD4/WC1-9WT, CD4/WC1-9Y24F, CD4/WC1-11WT, or CD4/WC1-11Y199F, showed that all cells could express IL-2 at equivalent levels (Fig. 6A).

When infected populations of Jurkat T cells bearing WT CD4/WC1 chimeric proteins were incubated with plate-bound anti-CD3 (TCR) plus anti-CD4 (WC1) Abs, an enhancement of IL-2 production was observed with all three types of WC1 endodomains above that are seen with anti-CD3 cross-linking alone (Fig. 6B). No IL-2 production over background occurred when cells were incubated with anti-CD4 alone, indicating that the WC1 signaling alone is not sufficient for T cell activation, but that it requires collaboration with signaling through the TCR/CD3 complex. Notably, cells expressing the WC1 type II Y24F or type III Y199F mutants and cross-linked with anti-CD3 plus anti-CD4 mAb costimulation showed no enhancement of IL-2 production. This indicates that the phosphorylation of Y_{24}EEL in WC1 type II endodomains, as in WC1 type I endomains, is required for WC1 to function as an activating coreceptor for TCR signaling and functional outcomes. It is of note that the lack of Y_{24}QEI phosphorylation in WC1 type III endodomains can be substituted by the phosphorylation of Y_{199}DDV, enabling WC1 type III endomains to potentiate T cell activation through the TCR.

Interestingly, the enhancement of IL-2 production varied among cells expressing the three different types of WC1 endodomains, with both the type II (WC1-9) and type III (WC1-11) WC1 endodomains resulting in significantly more IL-2 relative to that achieved with the type I endodomain (Fig. 6C).

Discussion

In previous studies, the 13 γδ T cell–specific WC1 molecules were classified into three types based on variation in endodomain sequences and the number of SRCR domains in the extracellular portion (16, 19). In this study, we focused on the endodomains and hypothesized that variation in the endodomain regions could play an important role in signal transduction differences, thus influencing the response of the $WC1^+$ γδ T cells following receptor ligation. We determined the sites of tyrosine phosphorylation in the type II (WC1-9) and type III (WC1-11) endodomain sequences and found that, whereas the type II was the same as the previously reported type I, tyrosine phosphorylation sites differed for the type III endodomain relative to the others. In addition, the time to reach the optimal level of phosphorylation when cross-linked to the TCR was more rapid for the type III endodomain, and cross-linking to the TCR resulted in the greatest IL-2 production when transduced Jurkat T cells were evaluated. Thus, all three endodomains deliver a stimulatory signal to the cells, although ligation of the ectodomains of type III WC1-11 could result in more rapid responses by those cells.

Ultimately, phosphorylation by src kinase family members is required for intracellular signaling events induced by the ligation

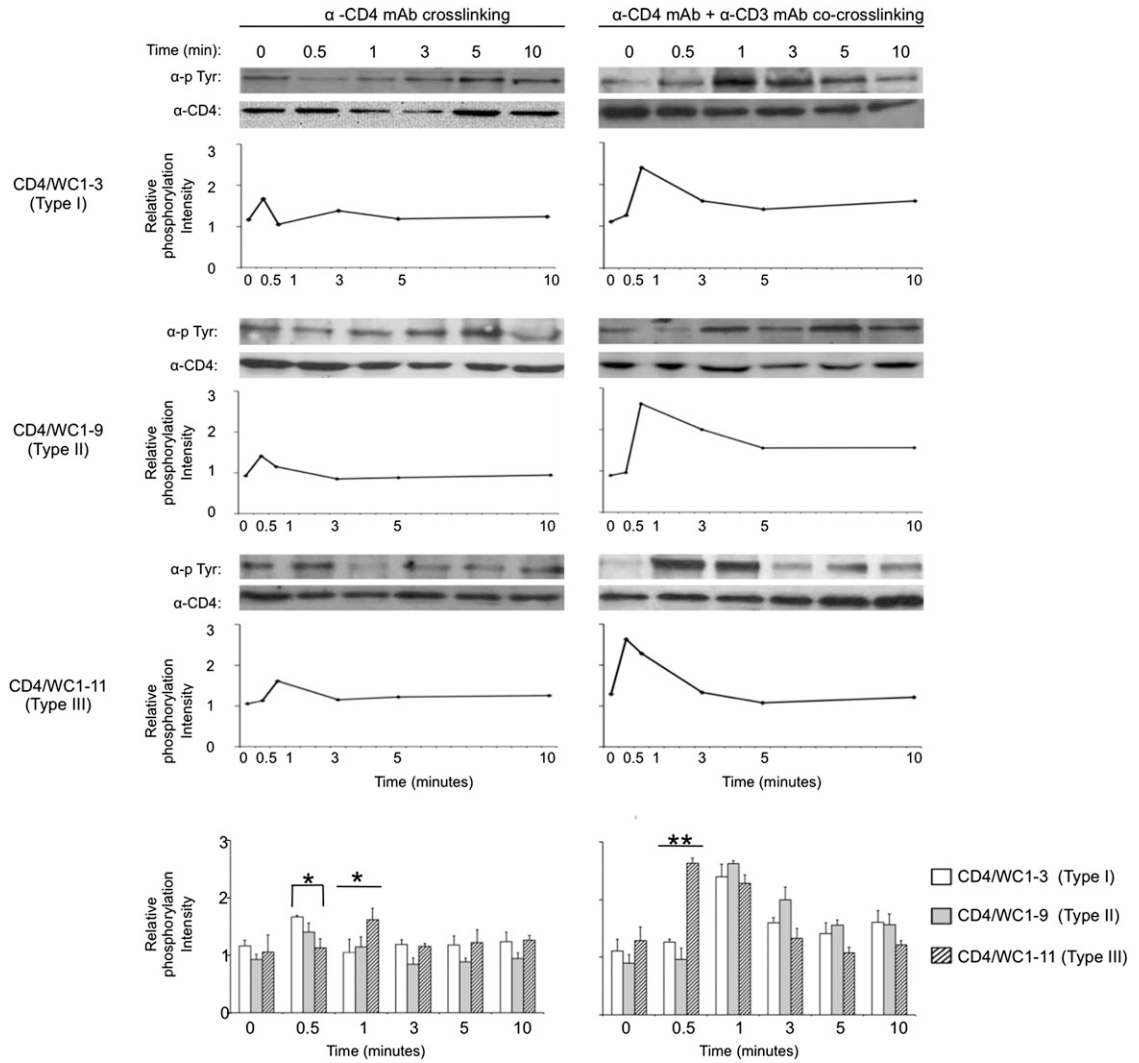

FIGURE 5. Kinetics of tyrosine phosphorylation varies depending upon the type of WC1 endodomain expressed. Jurkat T cells expressing CD4/WC1-3 (type I), CD4/WC1-9 (type II), or CD4/WC1-11 (type III) were cross-linked by anti-CD3 plus anti-CD4 or cross-linked with anti-CD4 alone. The intensity of phosphorylation at the indicated time points was normalized to the amount of CD4/WC1 chimeric protein and annotated as fold increase over the normalized phosphorylation intensity at the 0-min time point. The images shown are representative of at least two experiments. Bar graphs show the relative phosphorylation intensity of three different chimeric proteins (CD4/WC1-3, CD4/WC1-9, and CD4/WC1-11) at the indicated time points after cross-linking by anti-CD3 plus anti-CD4 mAb or cross-linking by anti-CD4 mAb alone. Values are means ± SD for three experiments. Significant differences ($p < 0.05$, one-way ANOVA with Bonferroni posttest) among the three different chimeric proteins are indicated by asterisks.

of cell accessory molecules in T cells (37). The models for WC1 phosphorylation by src kinases include other lymphocyte-associated accessory molecules, such as CD5 on T cells (38), FcR (39), and Igα and β on B cells (40). In this study, we identified the second and the last tyrosine residues as main targets of phosphorylation in the type II (*WC1-9*) and type III (*WC1-11*) endodomains, respectively, in a HEK-293 transfection system, and in stimulated and unstimulated Jurkat T cells. This extends previous studies showing that the second tyrosine residue of the type I (*WC1-3* and *WC1-4*) endodomains is phosphorylated by src family tyrosine kinases in vitro, in COS-7 and HEK-293 cotransfection systems, and in Jurkat T cells (17, 41). The association between WC1 and src family kinase members was shown previously by our laboratory by coimmunoprecipitation of those two components by either anti-src or anti-WC1 Ab (17). The responsibility of src family tyrosine kinases for the phosphorylation of the type I WC1 endodomain in $WC1^+$ γδ T cells was further confirmed by the observations that src family tyrosine kinases were constitutively expressed in HEK-293 cells and sorted $WC1^+$ γδ T cells and that cotransfection of members of src family tyrosine kinases enhanced phosphorylation levels of WC1 endodomains (17, 41). Because we applied the same HEK-293 transfection and Jurkat T cell systems to study the phosphorylation residues of the type II (*WC1-9*) and type III (*WC1-11*) endodomains, as done in the previous studies of the type I endodomains, it is likely that src family kinases account for the phosphorylation of the CD4/WC1-9 and CD4/WC1-11 chimeric proteins in those cells, although we did not directly evaluate this in this work.

Phosphorylation of only one tyrosine in the WC1 cytoplasmic domain is required for signaling. It is notable that phosphorylation of the last tyrosine (Y_{199}DDV) in the type III cytoplasmic domain functionally substitutes for the phosphorylation of the second tyrosine (Y_{24}EEL) in the type I and II endodomains. The second tyrosine in the type III (*WC1-11*) endodomain differs from that in the type I (WC1-3) and II (WC1-9) endodomains by the amino acid substitutions of glutamic acid to glutamine and leucine to isoleucine within the Y_{24}EEL motif. The resulting Y_{24}QEI motif in WC1-11 has been shown to be as readily phosphorylated by

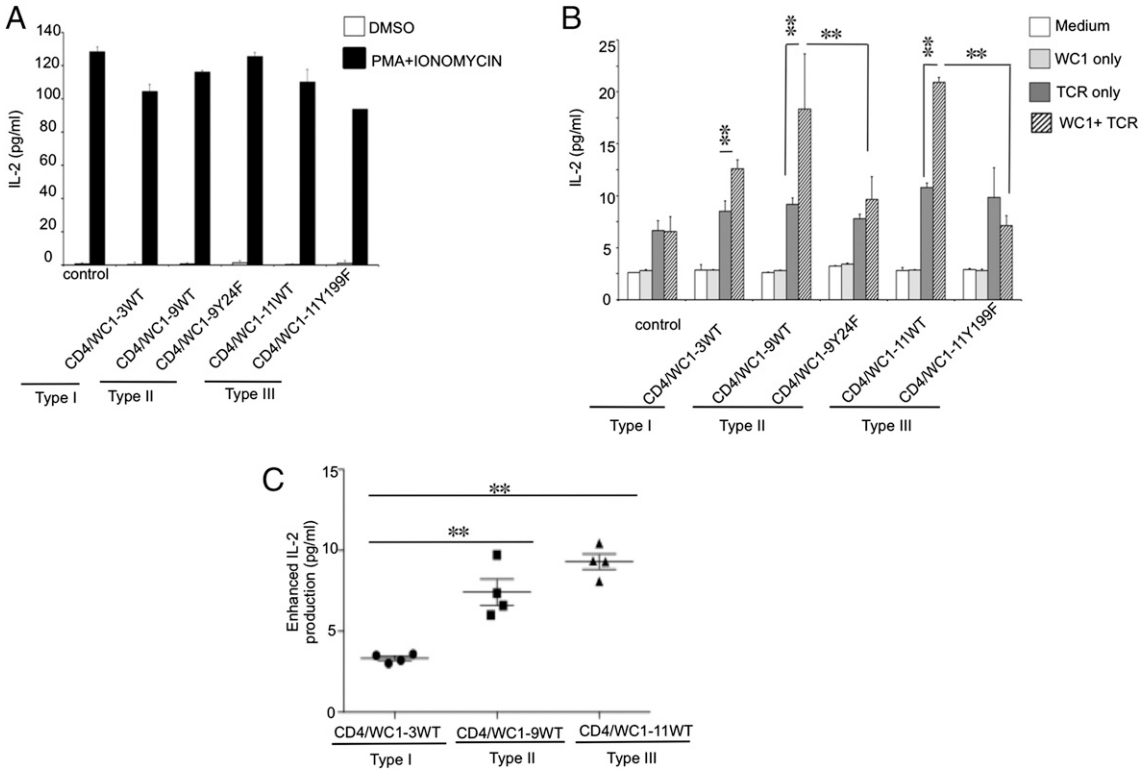

FIGURE 6. The enhancement of IL-2 production varies among Jurkat T cells expressing three different types of WC1 endodomains. Jurkat T cells (2×10^5) transduced with empty vector (control) or CD4/WC1 chimeric proteins were stimulated with PMA (50 ng/ul) and ionomycin (200 ng/ml) (**A**), or plate-bound anti-CD3 mAb (1 μg/ml) only, or plate-bound anti-CD3 (1 μg/ml) plus anti-CD4 mAb (5 ug/ml) for 48 h (**B** and **C**). IL-2 levels in supernatants were measured from triplicate cultures. Means ± SD for three independent experiments using populations of infected cells are plotted. Significant differences between WT CD4/WC1-transduced cells stimulated with anti-CD3 alone or by anti-CD3 and anti-CD4 or between WT CD4/WC1-transduced cells and mutant CD4/WC1 transduced stimulated by anti-CD3 and anti-CD4, as determined by a *t* test (two-tailed), are marked by asterisks ($p < 0.05$). (C) Enhanced IL-2 production is calculated by subtracting IL-2 production by control cells cross-linked with anti-CD3 plus anti-CD4 from IL-2 production by cells expressing CD4/WC1 proteins cross-linked with anti-CD3 plus anti-CD4. Significant differences between CD4/WC1-transduced cells stimulated with anti-CD3 and anti-CD4, as determined by a *t* test (two tailed), are marked by asterisks ($p < 0.05$).

tyrosine kinases as YEEL which, once phosphorylated, is bound tightly by the lck SH2 domain (42). In contrast, Y_{199}DDV is phosphorylated in WC1-11, but the same C-terminal Y_{138}DDV tyrosine motif is unphosphorylated in WC1-3 and WC1-4. A similar YDDI motif at the C terminus of WC1-9 is also unphosphorylated. Thus, the failure of Y_{24}QEI to be phosphorylated and the compensatory phosphorylation of Y_{199}DDV in WC1-11 are most likely due to a conformational change induced by the additional 80 aa that alters the accessibility of Y_{24}QEI and Y_{199}DDV.

SH2 domains from src tyrosine kinases and the adaptor protein Shc are the most likely binding partners for the phosphorylated Y_{24}EEL in type I and II endodomains (36). Recruiting Shc may signal to the Ras-MAPK or the PI3K/Akt pathways following WC1 activation, thereby increasing WC1$^+$ γδ T cell proliferation (43). Phosphorylated Y_{199}DDV in the type III endodomain would likely be bound by the SH2 domain of the adaptor proteins SLP-76 or Nck, which have been shown to bind to two phosphorylated YDDV motifs in ADAP (44–46). It remains to be determined whether phosphorylated Y_{24}EEL and Y_{199}DDV induce differential signals through the nucleation of different complexes or whether the phosphorylation of Y_{199}DDV in place of Y_{24}QEI in WC1-11 is an example of convergent evolution.

Because subpopulations of WC1$^+$ γδ T cells share a restricted set of expressed TCR-γ (TRGV3/TRGV7, TRGJ5-1/TRGJ5-2, and TRGC5) and TCR-δ (TRDJ1/TRDJ3) genes (22, 23) and differential WC1 gene expression correlates with the γδ T cell response to microbes, it is likely that the WC1 coreceptor plays an important determining role in γδ T cell functional responses. In this study, we showed that more than one WC1 gene product was expressed within a γδ T cell subpopulation and that within the Ab-defined WC1.1$^+$ population there are at least two subpopulations. One of those, the WC1.3$^+$ subpopulation, is defined by the mAb CACT21A, which reacts with WC1-8 only. However, upon flow cytometric sorting, we showed those cells also had *WC1-3* gene transcripts. WC1-3 is recognized by the WC1.1$^+$ subpopulation-defining mAb BAG25A, which does not recognize WC1-8. These subpopulations may account for functional divisions within the WC1.1$^+$ population. For example, a previous study by us showed that not all of the WC1.1$^+$ cells produced IFN-γ in response to *Leptospira* Ag (20). It remains to be determined whether functional differences within the WC1.1$^+$ subpopulation may be due to combinatorial expression of various WC1 molecules at a single-cell level. It is also important to note that, as we previously reported, WC1.2$^+$ cells respond more vigorously not only to Con A, as we repeated in this work, but to PMA plus ionomycin and to anti-CD3 Ab cross-linking. Also, WC1.2$^+$ cells do not decrease with aging the way WC1.1$^+$ cells do (20). Therefore, these two subpopulations may have more fundamental differences than just the expression of particular WC1 genes and responses to different pathogens.

WC1 coreceptors are similar to members of other PRR families based on the conservation of WC1 gene sequences among animals, the number of family members, and the potential to act as co-

stimulatory receptors for TCR signaling [as shown in this work and previously (17)]. This is supported by our recent evidence that WC1 molecules are needed for the response to *Leptospira* by γδ T cells, as shown by RNA silencing of WC1 molecules (21). Our observations that more than one WC1 molecule is expressed by a single cell is in line with the expression of multiple TLR on single cells, each of which interacts with unique ligands. Such diversity of PPRs on cells lends flexibility to their response, amplifying the stimulation through the TCR, as shown in this work. Our data show that ligation of the WC1 alone cannot induce activation of ex vivo cells [in this study and previously (17, 25)], although some tyrosine phosphorylation was found with the transduced Jurkat cells (17). The ability to reactivate previously activated lymphocytes through PRRs alone has been proposed, and some evidence is available for this (2).

Studies have shown that the activation of γδ T cells involves the upregulated expression of coreceptors, such as TLRs and NKRs, following functional differentiation of memory γδ T cells. As a costimulator, upregulated expression of NKG2D was observed in mouse γδ T cells in response to carcinoma cells (47, 48) and epithelial tumors (49). The engagement of TLRs by pathogen-associated molecular patterns upregulated the TLRs anchored in the cytoplasmic membranes of γδ T cells, which contributed to the magnified activation of γδ T cells in various infection models, such as *Escherichia coli*, *Mycobacterium tuberculosis*, and *Candida albicans* (50–52). Thus, it is possible that activation alters the expression levels of some WC1 molecules, and as such could facilitate either their role as a coreceptor or even as a direct receptor, although this activity is yet to be determined.

Disclosures

The authors have no financial conflicts of interest.

References

1. Bonneville, M., R. L. O'Brien, and W. K. Born. 2010. Gammadelta T cell effector functions: a blend of innate programming and acquired plasticity. *Nat. Rev. Immunol.* 10: 467–478.
2. Kawai, T., and S. Akira. 2010. The role of pattern-recognition receptors in innate immunity: update on Toll-like receptors. *Nat. Immunol.* 11: 373–384.
3. O'Neill, L. A., D. Golenbock, and A. G. Bowie. 2013. The history of Toll-like receptors: redefining innate immunity. *Nat. Rev. Immunol.* 13: 453–460.
4. Brennan, P. J., M. Brigl, and M. B. Brenner. 2013. Invariant natural killer T cells: an innate activation scheme linked to diverse effector functions. *Nat. Rev. Immunol.* 13: 101–117.
5. Olive, C. 2012. Pattern recognition receptors: sentinels in innate immunity and targets of new vaccine adjuvants. *Expert Rev. Vaccines* 11: 237–256.
6. Sarrias, M. R., J. Grønlund, O. Padilla, J. Madsen, U. Holmskov, and F. Lozano. 2004. The scavenger receptor cysteine-rich (SRCR) domain: an ancient and highly conserved protein module of the innate immune system. *Crit. Rev. Immunol.* 24: 1–37.
7. Brännström, A., M. Sankala, K. Tryggvason, and T. Pikkarainen. 2002. Arginine residues in domain V have a central role for bacteria-binding activity of macrophage scavenger receptor MARCO. *Biochem. Biophys. Res. Commun.* 290: 1462–1469.
8. Elomaa, O., M. Kangas, C. Sahlberg, J. Tuukkanen, R. Sormunen, A. Liakka, I. Thesleff, G. Kraal, and K. Tryggvason. 1995. Cloning of a novel bacteria-binding receptor structurally related to scavenger receptors and expressed in a subset of macrophages. *Cell* 80: 603–609.
9. Sarrias, M. R., S. Roselló, F. Sánchez-Barbero, J. M. Sierra, J. Vila, J. Yélamos, J. Vives, C. Casals, and F. Lozano. 2005. A role for human Sp alpha as a pattern recognition receptor. *J. Biol. Chem.* 280: 35391–35398.
10. Sarrias, M. R., M. Farnós, R. Mota, F. Sánchez-Barbero, A. Ibáñez, I. Gimferrer, J. Vera, R. Fenutría, C. Casals, J. Yélamos, and F. Lozano. 2007. CD6 binds to pathogen-associated molecular patterns and protects from LPS-induced septic shock. *Proc. Natl. Acad. Sci. USA* 104: 11724–11729.
11. Fabriek, B. O., R. van Bruggen, D. M. Deng, A. J. Ligtenberg, K. Nazmi, K. Schornagel, R. P. Vloet, C. D. Dijkstra, and T. K. van den Berg. 2009. The macrophage scavenger receptor CD163 functions as an innate immune sensor for bacteria. *Blood* 113: 887–892.
12. Bikker, F. J., A. J. Ligtenberg, C. End, M. Renner, S. Blaich, S. Lyer, R. Wittig, W. van't Hof, E. C. Veerman, K. Nazmi, et al. 2004. Bacteria binding by DMBT1/SAG/gp-340 is confined to the VEVLXXXXW motif in its scavenger receptor cysteine-rich domains. *J. Biol. Chem.* 279: 47699–47703.
13. Leito, J. T., A. J. Ligtenberg, K. Nazmi, J. M. de Blieck-Hogervorst, E. C. Veerman, and A. V. Nieuw Amerongen. 2008. A common binding motif for various bacteria of the bacteria-binding peptide SRCRP2 of DMBT1/gp-340/salivary agglutinin. *Biol. Chem.* 389: 1193–1200.
14. Vera, J., R. Fenutría, O. Cañadas, M. Figueras, R. Mota, M. R. Sarrias, D. L. Williams, C. Casals, J. Yelamos, and F. Lozano. 2009. The CD5 ectodomain interacts with conserved fungal cell wall components and protects from zymosan-induced septic shock-like syndrome. *Proc. Natl. Acad. Sci. USA* 106: 1506–1511.
15. Herzig, C. T., R. W. Waters, C. L. Baldwin, and J. C. Telfer. 2010. Evolution of the CD163 family and its relationship to the bovine gamma delta T cell co-receptor WC1. *BMC Evol. Biol.* 10: 181.
16. Herzig, C. T. A., and C. L. Baldwin. 2009. Genomic organization and classification of the bovine WC1 genes and expression by peripheral blood gamma delta T cells. *BMC Genomics* 10: 191.
17. Wang, F., C. Herzig, D. Ozer, C. L. Baldwin, and J. C. Telfer. 2009. Tyrosine phosphorylation of scavenger receptor cysteine-rich WC1 is required for the WC1-mediated potentiation of TCR-induced T-cell proliferation. *Eur. J. Immunol.* 39: 254–266.
18. Kisielow, J., M. Kopf, and K. Karjalainen. 2008. SCART scavenger receptors identify a novel subset of adult gammadelta T cells. *J. Immunol.* 181: 1710–1716.
19. Chen, C., C. T. Herzig, L. J. Alexander, J. W. Keele, T. G. McDaneld, J. C. Telfer, and C. L. Baldwin. 2012. Gene number determination and genetic polymorphism of the gamma delta T cell co-receptor WC1 genes. *BMC Genet.* 13: 86.
20. Rogers, A. N., D. G. Vanburen, E. E. Hedblom, M. E. Tilahun, J. C. Telfer, and C. L. Baldwin. 2005. Gammadelta T cell function varies with the expressed WC1 coreceptor. *J. Immunol.* 174: 3386–3393.
21. Wang, F., C. T. A. Herzig, C. Chen, H. Hsu, C. L. Baldwin, and J. C. Telfer. 2011. Scavenger receptor WC1 contributes to the γδ T cell response to Leptospira. *Mol. Immunol.* 48: 801–809.
22. Lahmers, K. K., J. Norimine, M. S. Abrahamsen, G. H. Palmer, and W. C. Brown. 2005. The CD4+ T cell immunodominant *Anaplasma marginale* major surface protein 2 stimulates gammadelta T cell clones that express unique T cell receptors. *J. Leukoc. Biol.* 77: 199–208.
23. Blumerman, S. L., C. T. Herzig, A. N. Rogers, J. C. Telfer, and C. L. Baldwin. 2006. Differential TCR gene usage between WC1− and WC1+ ruminant gammadelta T cell subpopulations including those responding to bacterial antigen. *Immunogenetics* 58: 680–692.
24. Herzig, C. T., M. P. Lefranc, and C. L. Baldwin. 2010. Annotation and classification of the bovine T cell receptor delta genes. *BMC Genomics* 11: 100.
25. Hanby-Flarida, M. D., O. J. Trask, T. J. Yang, and C. L. Baldwin. 1996. Modulation of WC1, a lineage-specific cell surface molecule of gamma/delta T cells augments cellular proliferation. *Immunology* 88: 116–123.
26. Minguet, S., M. Swamy, B. Alarcón, I. F. Luescher, and W. W. Schamel. 2007. Full activation of the T cell receptor requires both clustering and conformational changes at CD3. *Immunity* 26: 43–54.
27. Jin, Z. X., C. R. Huang, L. Dong, S. Goda, T. Kawanami, T. Sawaki, T. Sakai, X. P. Tong, Y. Masaki, T. Fukushima, et al. 2008. Impaired TCR signaling through dysfunction of lipid rafts in sphingomyelin synthase 1 (SMS1)-knockdown T cells. *Int. Immunol.* 20: 1427–1437.
28. Chenna, R., H. Sugawara, T. Koike, R. Lopez, T. J. Gibson, D. G. Higgins, and J. D. Thompson. 2003. Multiple sequence alignment with the Clustal series of programs. *Nucleic Acids Res.* 31: 3497–3500.
29. Hall, T. A. 1999. BioEdit: a user-friendly biological sequence alignment editor and analysis program for Windows 95/98/NT. *Nucl. Acids Symp. Ser.* 41: 95–98.
30. Baldwin, C. L., A. J. Teale, J. G. Naessens, B. M. Goddeeris, N. D. MacHugh, and W. I. Morrison. 1986. Characterization of a subset of bovine T lymphocytes that express BoT4 by monoclonal antibodies and function: similarity to lymphocytes defined by human T4 and murine L3T4. *J. Immunol.* 136: 4385–4391.
31. Morrison, W. I., and W. C. Davis. 1991. Individual antigens of cattle: differentiation antigens expressed predominantly on CD4− CD8− T lymphocytes (WC1, WC2). *Vet. Immunol. Immunopathol.* 27: 71–76.
32. Wijngaard, P. L., N. D. MacHugh, M. J. Metzelaar, S. Romberg, A. Bensaid, L. Pepin, W. C. Davis, and H. C. Clevers. 1994. Members of the novel WC1 gene family are differentially expressed on subsets of bovine CD4−CD8− gamma delta T lymphocytes. *J. Immunol.* 152: 3476–3482.
33. Larkin, M. A., G. Blackshields, N. P. Brown, R. Chenna, P. A. McGettigan, H. McWilliam, F. Valentin, I. M. Wallace, A. Wilm, R. Lopez, et al. 2007. Clustal W and Clustal X version 2.0. *Bioinformatics* 23: 2947–2948.
34. Kanan, J. H., N. Nayeem, R. M. Binns, and B. M. Chain. 1997. Mechanisms for variability in a member of the scavenger-receptor cysteine-rich superfamily. *Immunogenetics* 46: 276–282.
35. Chen, C., C. T. A. Herzig, J. C. Telfer, and C. L. Baldwin. 2009. Antigenic basis of diversity in the gammadelta T cell co-receptor WC1 family. *Mol. Immunol.* 46: 2565–2575.
36. Songyang, Z., S. E. Shoelson, J. McGlade, P. Olivier, T. Pawson, X. R. Bustelo, M. Barbacid, H. Sabe, H. Hanafusa, T. Yi, et al. 1994. Specific motifs recognized by the SH2 domains of Csk, 3BP2, fps/fes, GRB-2, HCP, SHC, Syk, and Vav. *Mol. Cell. Biol.* 14: 2777–2785.
37. Mustelin, T., and K. Taskén. 2003. Positive and negative regulation of T-cell activation through kinases and phosphatases. *Biochem. J.* 371: 15–27.
38. Raab, M., M. Yamamoto, and C. E. Rudd. 1994. The T-cell antigen CD5 acts as a receptor and substrate for the protein-tyrosine kinase p56lck. *Mol. Cell. Biol.* 14: 2862–2870.

39. Pasquier, B., P. Launay, Y. Kanamaru, I. C. Moura, S. Pfirsch, C. Ruffié, D. Hénin, M. Benhamou, M. Pretolani, U. Blank, and R. C. Monteiro. 2005. Identification of FcalphaRI as an inhibitory receptor that controls inflammation: dual role of FcRgamma ITAM. *Immunity* 22: 31–42.
40. DeFranco, A. L., J. D. Richards, J. H. Blum, T. L. Stevens, D. A. Law, V. W. Chan, S. K. Datta, S. P. Foy, S. L. Hourihane, M. R. Gold, et al. 1995. Signal transduction by the B-cell antigen receptor. *Ann. N. Y. Acad. Sci.* 766: 195–201.
41. Pillai, M. R., E. A. Lefevre, B. V. Carr, B. Charleston, and P. O'Grady. 2007. Workshop cluster 1, a gammadelta T cell specific receptor is phosphorylated and down regulated by activation induced Src family kinase activity. *Mol. Immunol.* 44: 1691–1703.
42. Nika, K., L. Tautz, Y. Arimura, T. Vang, S. Williams, and T. Mustelin. 2007. A weak Lck tail bite is necessary for Lck function in T cell antigen receptor signaling. *J. Biol. Chem.* 282: 36000–36009.
43. Gu, H., H. Maeda, J. J. Moon, J. D. Lord, M. Yoakim, B. H. Nelson, and B. G. Neel. 2000. New role for Shc in activation of the phosphatidylinositol 3-kinase/Akt pathway. *Mol. Cell. Biol.* 20: 7109–7120.
44. Geng, L., M. Raab, and C. E. Rudd. 1999. Cutting edge: SLP-76 cooperativity with FYB/FYN-T in the up-regulation of TCR-driven IL-2 transcription requires SLP-76 binding to FYB at Tyr595 and Tyr651. *J. Immunol.* 163: 5753–5757.
45. Raab, M., H. Kang, A. da Silva, X. Zhu, and C. E. Rudd. 1999. FYN-T-FYB-SLP-76 interactions define a T-cell receptor zeta/CD3-mediated tyrosine phosphorylation pathway that up-regulates interleukin 2 transcription in T-cells. *J. Biol. Chem.* 274: 21170–21179.
46. Sylvester, M., S. Kliche, S. Lange, S. Geithner, C. Klemm, A. Schlosser, A. Grossmann, U. Stelzl, B. Schraven, E. Krause, and C. Freund. 2010. Adhesion and degranulation promoting adapter protein (ADAP) is a central hub for phosphotyrosine-mediated interactions in T cells. *PLoS One* 5: e11708.
47. Corvaisier, M., A. Moreau-Aubry, E. Diez, J. Bennouna, J. F. Mosnier, E. Scotet, M. Bonneville, and F. Jotereau. 2005. V gamma 9V delta 2 T cell response to colon carcinoma cells. *J. Immunol.* 175: 5481–5488.
48. Viey, E., G. Fromont, B. Escudier, Y. Morel, S. Da Rocha, S. Chouaib, and A. Caignard. 2005. Phosphostim-activated gamma delta T cells kill autologous metastatic renal cell carcinoma. *J. Immunol.* 174: 1338–1347.
49. Girardi, M., D. E. Oppenheim, C. R. Steele, J. M. Lewis, E. Glusac, R. Filler, P. Hobby, B. Sutton, R. E. Tigelaar, and A. C. Hayday. 2001. Regulation of cutaneous malignancy by gammadelta T cells. *Science* 294: 605–609.
50. Cui, Y., L. Kang, L. Cui, and W. He. 2009. Human gammadelta T cell recognition of lipid A is predominately presented by CD1b or CD1c on dendritic cells. *Biol. Direct* 4: 47.
51. Martin, B., K. Hirota, D. J. Cua, B. Stockinger, and M. Veldhoen. 2009. Interleukin-17-producing gammadelta T cells selectively expand in response to pathogen products and environmental signals. *Immunity* 31: 321–330.
52. Shibata, K., H. Yamada, H. Hara, K. Kishihara, and Y. Yoshikai. 2007. Resident Vdelta1+ gammadelta T cells control early infiltration of neutrophils after *Escherichia coli* infection via IL-17 production. *J. Immunol.* 178: 4466–4472.